prediction of radiation-induced changes in lung density on follow-up CT can be of help with differential diagnosis. The goal of this work was to develop a Normal Tissue Complication Probability (NTCP) model for voxel by voxel prediction of changes in lung density on CT scans of patients treated with IMRT.

Material and Methods: 20 patients were treated with fractionated IMRT (60 Gy/25 fractions) or SBRT with Helical Tomotherapy (40-52 Gy in 5-10 fractions) for lung tumors.Follow-up CT scans were acquired at 6 months after the end of RT and were registered with pre-treatment scans using rigid (6 degrees of freedom) followed by a b-spline (> 27 degrees of freedom) deformable registration performed using the 3D Slicer freeware software suite. Registration accuracy was assessed by comparing the calculated displacement at bifurcation points with the displacement measured on unregistered images. Registration was repeated when the difference was more than 1 cm. Voxels Hounsfield units were converted into relative electron density (RED) using in-phantom measured CT-RED curves. The change in RED between the two images was calculated for each voxel within the healthy lung tissue, defined as combined lungs after subtraction of PTV, among all the patients. Voxels RED changes versus absolute dose were fitted among all patients using a function similar to Lyman NTCP model. Model parameters were *D0.5*, the dose giving 0.5 increase in relative electron density and *m*, the slope of the dose-response curve. No correction was used for fractionation of the treatments. Predictive power of model was assessed by a test of correlation of measured and predicted RED changes.

Results: The dose giving an increase of 0.5 RED estimated from fitting of lung density changes was *D0.5* = 99.5 Gy (95%CI = 84.0-114.9 Gy). Slope of dose response, *m*, was 0.338 (95%CI = 0.296-0.380). The correlation test shows that predicted and measured RED changes were statistically strongly correlated ($p<0.001$).

Conclusion: The model describes well the change in RED in follow-up CT scans of IMRT patients and can be used to generate maps of predicted RED to be visualized on follow-up CT scans, as a support for differential diagnosis between benign changes from progression or recurrence.

PO-0877

Baseline CT image and isodose shape features improve prognostic models for dyspnea after RT in NSCLC

G. Defraene[1], W. Van Elmpt[2], D. De Ruysscher[3]
[1]*KU Leuven - University of Leuven, Experimental Radiation Oncology, Leuven, Belgium*
[2]*Maastricht University Medical Centre, Department of Radiation Oncology Maastro-Clinic, Maastricht, The Netherlands*
[3]*University Hospitals Leuven, Department of Radiation Oncology, Leuven, Belgium*

Purpose or Objective: Lung toxicity prediction models currently rely on dosimetric factors as mean lung dose (MLD) or V20 (volume of lung receiving more than 20 Gy), and clinical factors (e.g. age, smoking history). With a consistently reported area under the curve (AUC) around 0.6 these models are limited in discriminating between low- and high-risk patients before treatment. The present study aims at designing a better prognostic model by broadening the search for prognostic factors using a radiomics approach both on the imaging and dosimetric level. For this, CT image features of lung tissue and isodose shape measures were explored to predict the endpoint of dyspnea.

Material and Methods: 80 stage I-IV non-small cell lung cancer patients were included. Prescription dose was 66Gy, in fractions of 2.75 Gy sequentially or 2 Gy concurrent with chemotherapy. Maximal increase in CTCAE 4.0 dyspnea score in the first 6 months after the end of radiotherapy was retrospectively recorded with respect to baseline status.
30 lung image features were extracted from the baseline free-breathing planning CT: 10 intensity-based features (derived from the histogram of intensities), and the mean value and standard deviation of 10 texture features (from the co-occurrence matrix, neighbourhood gray tone difference matrix (NGTDM) and neighbouring gray level dependence matrix (NGLDM) categories). All features were calculated within each of the isodose volumes V5, V20 and V40 of the lung excluding the GTV structure. Additionally 15 shape and location features of these isodose volumes were collected: volume, bounding box dimensions, centroid coordinates and compactness. Other features included age, smoking status, chemotherapy regimen, treatment modulation, heart Dmax and Dmean.
All combinations of the 5 most significant features resulting from a univariate logistic regression analysis were tested in multivariate setting (likelihood ratio test between nested models).

Results: Dyspnea increase grade >= 2 was present in 13.8% of patients. For an increase of at least 1 grade, this was 38.8%.
In univariate modeling, several image and isodose shape features performed significantly better than MLD for both endpoints (Table 1). The resulting classifier for dyspnea increase grade >= 1 was based on the texture feature 'small number emphasis' and the V40 isodose antero-posterior dimension (AUC=0.71). The dyspnea increase grade >= 2 classifier was based on mean heart dose and antero-posterior dimension of the V20 isodose (AUC=0.71).

Feature	AUC
Dyspnea increase grade ≥1	
Texture small number emphasis (NGLDM): mean in V_{20}*	0.66
Texture small number emphasis (NGLDM): SD in V_{20}	0.66
Texture Deviation: mean in V_{20}	0.63
Shape: V_{40} bounding box relative antero-posterior dimension*	0.62
Intensity histogram in V_{20}: 75th quantile	0.60
Mean Lung Dose	*0.51*
Dyspnea increase grade ≥2	
Texture Strength (NGTDM): mean in V_{40}	0.70
Texture Coarseness (NGTDM): mean in V_{20}	0.69
Texture Complexity (NGTDM): mean in V_{20}	0.67
Mean heart dose*	0.66
Shape: V_{20} bounding box absolute antero-posterior dimension*	0.65
Mean Lung Dose	*0.57*

*selected as covariate in the best multivariate model

Table 1 Area under the curve (AUC) of univariate logistic regression models for the 5 most prognostic features. A mean lung dose-based model performance is given as reference.

Conclusion: A radiomics analysis with image and isodose features yielded promising prognostic models for dyspnea compared to the classical MLD-based model. Validation on a recently available large multicentric database will be performed by the time of the congress, which will allow the selection of the most robust model.
This project has received funding from the European Union's Seventh Framework Programme under grant agreement no 601826 (REQUITE).

Poster: Physics track: Intra-fraction motion management

PO-0878

The effect of rectal retractor on intra-fraction motion of prostate

A. Vanhanen[1,2], M. Kapanen[1,2]
[1]*Tampere University Hospital, Department of Oncology, Tampere, Finland*
[2]*Medical Imaging Center and Hospital Pharmacy, Medical Physics, Tampere, Finland*

Purpose or Objective: Intra-fraction motion of the prostate is a known phenomenon that degrades the delivered dose to

the target. Rectal retractor (RF) which main purpose is to separate the rectum from the prostate in order to decrease the rectal dose is commonly suggested to fixate the prostate [1]. In the current study the effect of RF on intra-fraction motion of the prostate was investigated using real-time electromagnetic tracking system.

Material and Methods: A total of 22 conventionally fractionated (39 x 2 Gy) or moderately hypofractionated (20 x 3 Gy) prostate cancer patients were investigated. RF (RectafixTM, Scanflex Medical AB, Sweden) was used in 15/39 and 10/20 first fractions to study its effect on prostate motion. In the RF method the rectum-prostate separation is achieved by rectal rod that is inserted into the rectum and manually pushed posteriorly. Intra-fraction motion of the prostate was recorded with electromagnetic tracking system RayPilot (Micropos Medical AB, Sweden). The system consists of a transmitter implanted into the prostate and a receiver plate positioned on the treatment couch. The system provides transmitter 3D position in real-time. Intra-fractional prostate motion of a total of 260 RF fractions and 351 non-RF fractions were tracked and analyzed. Absolute prostate displacement after image guidance was calculated in all directions. Unidirectional and 3D motion distributions within 10 min treatment time were evaluated by the means of percentage time at displacement≥ 1, 2, 3, 4, 5 and 6 mm. Motion patterns between the RF and non-RF fractions were compared individually and over the whole patient population.

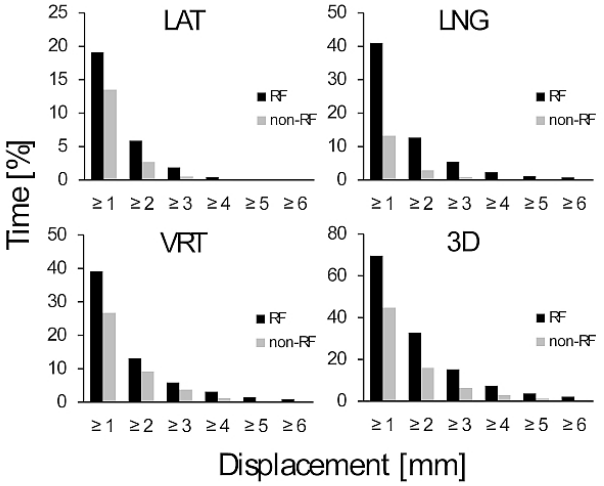

Figure 1. Average percentage time of lat, lng, vrt and 3D prostate displacements

Results: The average percentage time was larger in RF data compared to non-RF data in every direction (fig 1). The greatest increase in motion was seen in superior, inferior and posterior directions (table 1). Differences between the datasets in these directions, as well as 3D motion, were statistically significant ($p < 0.03$). Individually, the 3D motion of the prostate was significantly larger ($p < 0.05$) with RF than without it for 13 patients. For two patients significant ($p \leq 0.04$) stabilizing effect with the RF was observed.

Table 1. Average percentage time of unidirectional and 3D prostate displacements ≥ 1, 2, 3, 4, 5 and 6 mm

		≥1	≥2	≥3	≥4	≥5	≥6
3D	RF	69,6	32,8	15,3	7,5	3,8	2,2
	non-RF	44,8	16,0	6,4	2,9	1,4	0,5
Left	RF	9,4	3,5	1,6	0,4	0,0	0,0
	non-RF	7,5	1,8	0,5	0,2	0,0	0,0
Right	RF	9,7	2,4	0,3	0,1	0,0	0,0
	non-RF	6,0	0,9	0,1	0,0	0,0	0,0
Superior	RF	6,0	2,4	1,1	0,3	0,1	0,0
	non-RF	3,8	1,5	0,6	0,1	0,0	0,0
Inferior	RF	35,0	10,3	4,4	2,0	1,0	0,8
	non-RF	9,4	1,4	0,3	0,0	0,0	0,0
Anterior	RF	8,6	4,1	2,1	0,9	0,2	0,1
	non-RF	9,3	3,6	1,5	0,8	0,4	0,2
Posterior	RF	30,5	9,1	3,8	2,3	1,3	0,9
	non-RF	17,5	5,6	2,2	0,4	0,1	0,0

Conclusion: The use of RF increased the intra-fraction motion of the prostate on average and for most of the patients. The reason for larger motion could be increased muscular tension due to uncomfortableness of the RF and the anatomical changes that the retraction creates at the prostate-rectum surface. Our results indicate that the use of RF requires larger treatment margins or application of real-time tracking and dose gating. As the RF increases the prostate motion its use is questionable and should be evaluated against desired rectum dose sparing.

References:

[1] Nicolae A. et al. Radiat Oncol (2015) 10:122

PO-0879

Real-time prostate tracking in prostate cancer radiotherapy using autoscan transperineal ultrasound

X. Qi[1], X.S. Gao[1], H. Yu[1], S.B. Qin[1], H.Z. Li[1]
[1]*Peking University First Hospital, Radiation Oncology, Beijing, China*

Purpose or Objective: More recently, noninvasive 4D transperineal ultrasound (4D-TPUS) has been introduced in tracking interfraction, as well as intrafraction prostate motion in radiotherapy. Compared to other tracking method, the ultrasound has its own advantage in precise identification of soft tissue without invasive procedure or extra radiation dose. Several studies have reported the tracking data that confirming its accuracy in monitoring prostate motion and 4D-TPUS is nowadays gradually accepted as a monitoring option in prostate cancer radiotherapy. However, rare experience of this new technology with Asia populations has been reported. In this study, we report our clinical experience and tracking data using 4D-TPUS to monitor both inter- and intra-fraction prostate motion.

Material and Methods: Fifteen prostate cancer patients were enrolled in a prospective study and treated to a total dose of 76Gy in 38 fractions using IMRT. For each patient, before treatment delivery, prostates were localized using US and CBCT respectively to determine setup offsets relative to the patient skin tattoos. In the treatment protocol, adjustment of couch was guided by CBCT images. During the treatment, real-time ultrasound images were acquired and data was collected for direct monitoring of 3D motion of the prostate.

Results: A total of 221 fractions were evaluated. The means (μ) and standard deviations (SD) of inter-fraction prostate motion, as evaluated using CBCT and US, averaged from all patients and fractions, were [μ US = (4.62, 4.75, 4.37) mm, SD US = (4.21, 5.17, 5.52) mm], and [μ CBCT = (2.49, 2.26, 3.27) mm, SD CBCT = (2.15, 1.83, 2.89) mm] in the left-right, superior-inferior and anterior-posterior directions, respectively. The median (5% to 95% percentile) of 221 intra-fraction prostate motions in the L−/R+, S+/I− and A+/P− were